EUROPEAN FUSION DEVELOPMENT AGREEMENT

EFDA–JET–CP(01)02-55

A. Huber, P. Coad, D. Coster, L.C. Ingesson, G.F. Matthews, Ph. Mertens,
V. Philipps, A. Pospieszczyk, B. Schweer, G. Sergienko, M. Stamp, K. Itami
and JET EFDA Contributors

Reconstruction of 2-D line Radiation Distributions in the JET MkIIGB Divertor Using CCD Camera Tomography

Reconstruction of 2-D line Radiation Distributions in the JET MkIIGB Divertor Using CCD Camera Tomography

A.Huber[1], P.Coad[2], D.Coster[3], L.C.Ingesson[4], G.F.Matthews[2], Ph.Mertens[1], V.Philipps[1], A.Pospieszczyk[1], B.Schweer[1], G.Sergienko[5], M.Stamp[2], K.Itami[6] and JET EFDA Contributors*

[1]Institut für Plasmaphysik, Forschungszentrum Jülich GmbH, EURATOM Association, Trilateral Euregio Cluster, D-52425 Jülich, Germany,
[2]Euratom/UKAEA Fusion Association, Culham Science Centre, Abingdon, Oxon OX14 3DB,UK,
[3]Max-Planck-Institut für Plasmaphysik, Garching,
[4]FOM-Instituut voor Plasmafysica, Nieuwegein, The Netherlands,
[5]Institute of High Temperatures, Russian Academy of Sciences, Moscow, Russian Federation,
[6]Japan Atomic Energy Research Institute, Naka-machi, Ibaraki-ken, Japan 311-0193
**See appendix of the paper by J.Pamela "Overview of recent JET results", Proceedings of the IAEA conference on Fusion Energy, Sorrento 2000*

Preprint of Paper to be submitted for publication in Proceedings of the EPS Conference,
(Madeira, Portugal 18-22 June 2001)

‘‘This document is intended for publication in the open literature. It is made available on the understanding that it may not be further circulated and extracts or references may not be published prior to publication of the original when applicable, or without the consent of the Publications Officer, EFDA, Culham Science Centre, Abingdon, Oxon, OX14 3DB, UK.”

“Enquiries about Copyright and reproduction should be addressed to the Publications Officer, EFDA, Culham Science Centre, Abingdon, Oxon, OX14 3DB, UK.”

INTRODUCTION

The amount and spatial distribution of impurity radiation in the divertor of a tokamak is of fundamental importance for the behaviour of power exhaust, detachment, recombination, recycling and erosion/redeposition properties. Carbon impurity radiation in the divertor is indispensable to reduce the peak heat flux to the strike zones but carbon erosion also limits the lifetime of the target and leads to large tritium retention via co-deposition. In addition to line-integrated spectroscopic measurements, spatially resolved radiation of the various species obtained from tomographic inversion of 2D-CCD camera data is an important tool for diagnosing the role of impurity and hydrogen radiation in the divertor physics.

1. EXPERIMENTAL SETUP AND PRINCIPLE OF TOMOGRAPHIC INVERSION

At JET, three CCD cameras (KL1 camera diagnostic, dynamical range of 8 bits, CCD-chip with 582x752 pixels) view the divertor in a nearly tangential geometry. They are coupled with interference filters and allow measurement of line-emission at three wavelengths (e.g. D_α, CII, CIII simultaneously). The images are recorded by three video recorder at a rate of 50 half frames per second. Concurrently, video signals are captured from cameras with a framegrabber board, which transfers images directly into the main memory.

The Fig.1a. displays the projections of lines of sight of the cameras into a poloidal plane showing only a reduced amount of chords (every 30 chord). There are enough chords in the whole divertor region to resolve the emission pattern along the radial direction with sufficent resolution but the resolution in z-direction (vertically) is limited due to the small number of chords crossing each other with large angle. Figure1b. illustrates the lines of sight for eight locations selected in the divertor region, showing only the chords passing through these points. Since the range of angles between the lines of sight is smaller than 40 degrees, the resolution in the z-direction is limited.

The evaluation of the 2D-emission distribution in a poloidal plane assu-mes toroidal symmetry and is obtained by sol-ving the matrix equation $Ax = b$ using the Singular Value Decomposition method[1]. Here, A is the "geometry matrix" that contains the geometric information about the view of each CCD-pixel and the divertor structures limiting the corresponding lines of sight. The vector b contains the raw data (digitised CCD data), x is the solution. The Singular Value Decomposition (SVD) method decomposes the MxN (M number of lines of sight, N number of divertor cells) matrix A into three matrixes $A = UwV^T$Ä, where U is an MxN column orthogonal matrix, V^T is the transpose of an NxN orthogonal matrix, and w is an NxN diagonal matrix with nonnegative elements. The w matrix represents the singularity of the "geometry matrix". When M>N, the solution in the sense of minimising |Ax-b|, is given by $x = V\ 1/w\ U^T b$ where 1/w is the inverse of the NxN diagonal matrix, for which, however, zero and small value elements are removed. The tolerance ($TOL = w_{i\ min} / w_{i\ max}$), defines the minimum w_i in 1/w. To define the optimal tolerance, phantom studies have been performed using several "test distributions" as input. Figure 2a. shows as an example a radiation profile of the form $x^p(z, r) = \sum_{i=1, 2} 1000.00 \times \exp((\frac{r\text{-}ri}{l})^2)$, l = 7cm, aiming to simulate a toroidally elongated radiation source in the divertior region. Using the "geometry

matrix" the virtual video image b^v can be easily calculated ($b^v = Ax^p$) and used as input for tomographic inversion. The result of this inversion with a optimised tolerance of 0.03 is shown in Fig.2b. The optimised tolerance of 0.03 was found by choosing the minimum of the tomographical error $\sigma_{tomo} = \{\sum_i (x_i - x^p_i)^2\}^{1/2}/\{\sum_i (x^p_i)^2\}^{1/2} = 0.5$ and the smallest reconstruction error $\sigma_{rec} = \{\sum_i (b_i - (Ax)_i^2\}^{1/2}/\{\sum_i (b_i)^2\}^{1/2} < 0.035$) for our geometry. Due to the limited re-solution in z-direction, the 2D reconstructed emission in the z-direction is enlarged ($\approx 5cm$).

2. RESULTS AND DISCUSSION

L-mode Experiments have been performed with $B_T = 2.4T$ and $I_p = 2MA$ at an averaged central electron density of $\overline{n}_e \approx 3\times10^{19}m^{-3}$ and with additional NBI power of 1.85MW. The divertor strike points are moved along the vertical targets and the fixed Langmuir probes at about constant plasma density. The Fig. 3a shows the time evolution of inner strike point (ISP) location (z-coordinate) and the saturation currents of the probes 3,4 and 5 shown in Fig. 3b which are maximal when the inner strike point is located on the corresponding probe (19.18s on probe 5 and 19.32s on probe 4). Fig.4 shows the camera images of D_α- (a) and CIII-emissions (e) in the divertor together with the reconstructed images for D_α- (b) and CIII-emissions (f) and the 2D solutions of the D_α- (c) and CIII-emissions (g) at a time of t = 19.18s. Figure 4d and (h) show the 2D solutions of D_α- and CIII-emissions at a time of t = 19.32s, where the strike point is moved up. As can be seen, the spatial location of the strike point obtained by the tomographical reconstruction correlates well with probe measurements of the ion saturation current. Thus, under attached conditions, the maximum of the hydrogen radiation is located always near the target plates at the position of the strike zones (at t = 19.18s at location of probe 5 and t = 19.32s at probe 4) but with a strong in-out asymmetry showing about a factor 2-5 more hydrogen radiation at the inner divertor leg. The reconstructed video images from the D_α- and CIII-emissions have a reconstruction error which is smaller than 0.04. As can be also seen, the CIII-radiation shows an opposite in-out asymmetry behaviour with the strongest CIII-emission located in the outer divertor leg. Strong CIII-radiation is also observed near the X-point for these L-mode attached plasma conditions.

The reconstructed D_α-emission profiles have been compared with the line integrated emission of D_α-hydrogen line radiation measured vertically from the top of the machine by an absolutely calibrated CCD camera array. As can be seen in Fig.5, the reconstructed poloidal D_α-emission profiles match the data from the camera array very well. It should be also mentioned, that the comparison between SVD (presented here) and Non-Negativity Constraint (used for radiation tomography) [2,3] is in good agreement.

SUMMARY AND CONCLUSION.

2D emission profiles of CIII and D_α radiation in the JET Divertor have been reconstructed by the Singular Value Decomposition method to obtain the emission pattern in a poloidal plane. In this

contribution, L-mode conditions with the strike points moved along the vertical target plates have been analysed. The spatial location of the strike points obtained by tomographical reconstruction correlates well with the ion saturation current of the fixed target Langmuir probes. Under the attached conditions investigated, the maximum of the hydrogen radiation is located near the target plates at the position of the strike zone but with significantly more radiation from the inner leg compared with to the outer. The CIII-radiation is much stronger in the outer divertor with a strong contribution near the X-point. A good agreement between the emission pattern obtained from the different diagnostics is obtained. Also, the comparison between SVD and Non-Negativity Constraint Method shows good correlation.

REFERENCES

[1]. G.H.Golub and C.F. Van Loan, John Hopkins University Press, Baltimore, 1983.

[2]. L.C.Ingesson et al., Nucl. Fusion **3**8, 1675 (1998).

[3]. L.C.Ingesson et al., this conference.

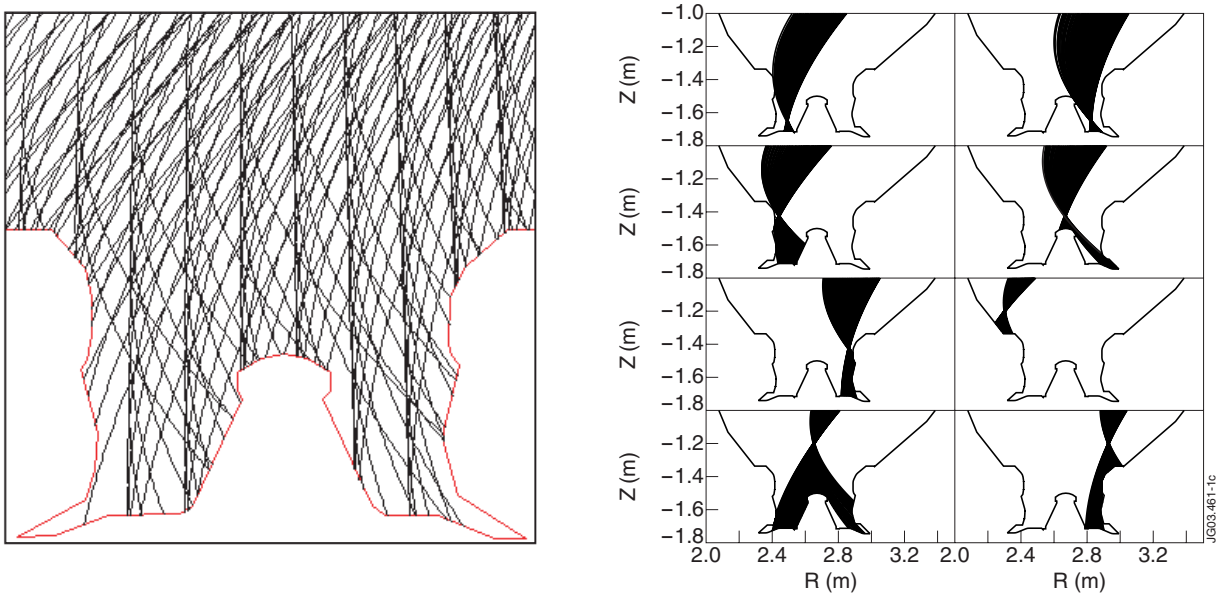

Figure 1: Projections of lines of sight of KL1 cameras into a poloidal plane.

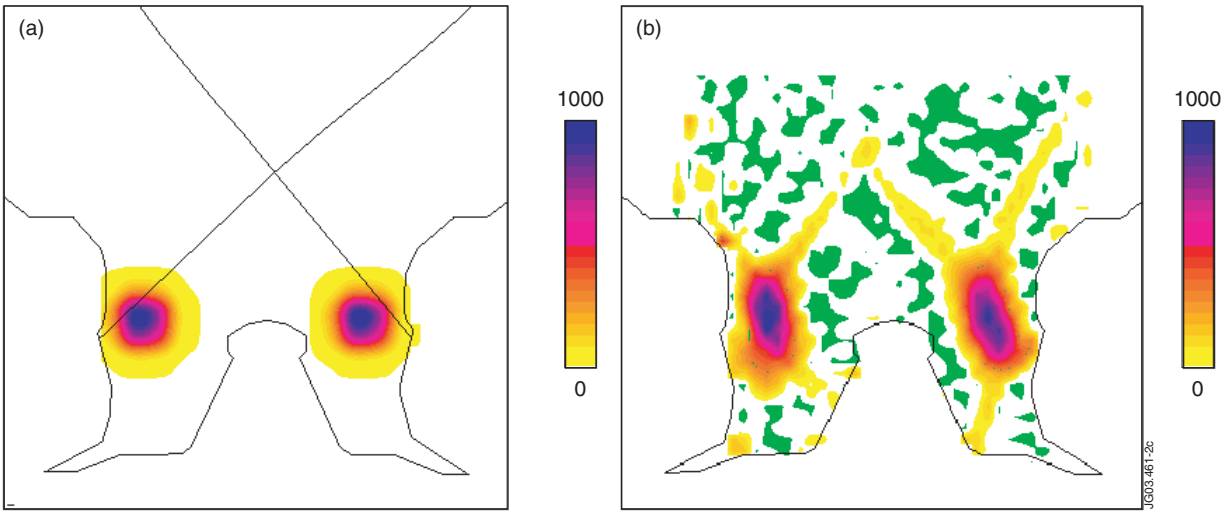

Figure 2: Reconstruction of a phantom distribution function: a) the original distribution; b) reconstruction with TOL = 0.03.

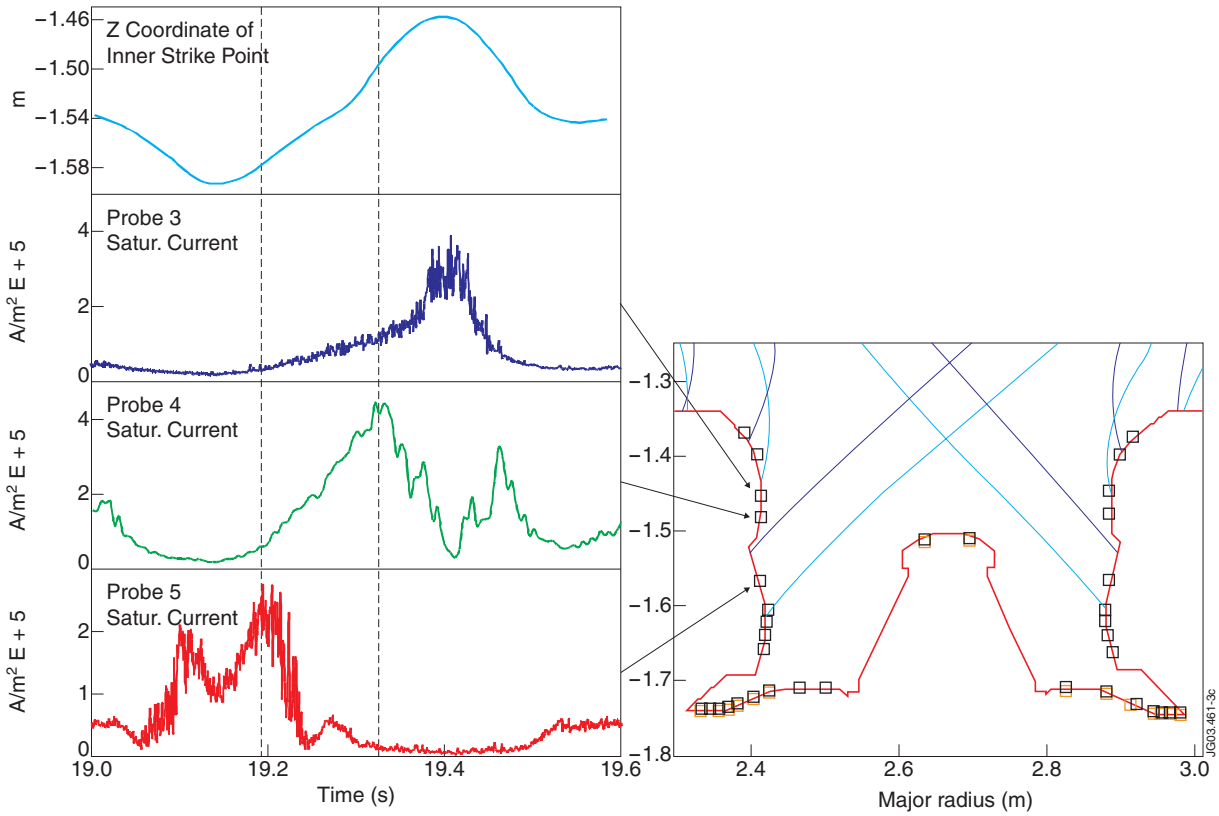

Figure 3: Time evolution of inner strike-point position and saturation current of probes in inner divertor.

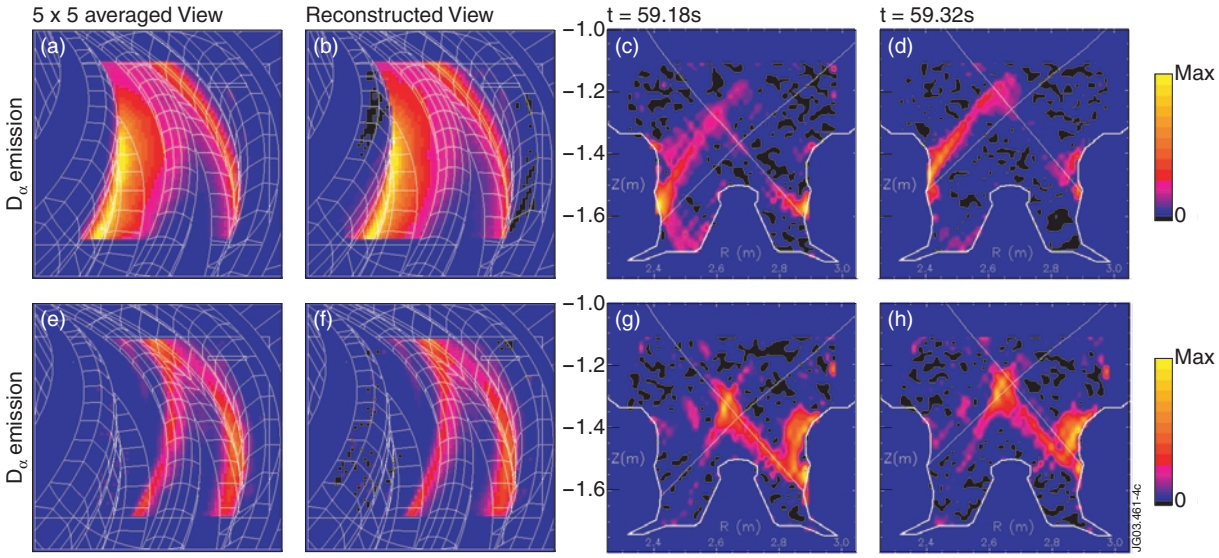

Figure 4:D_α- and CIII-emissions in the divertor (see explanation in text).

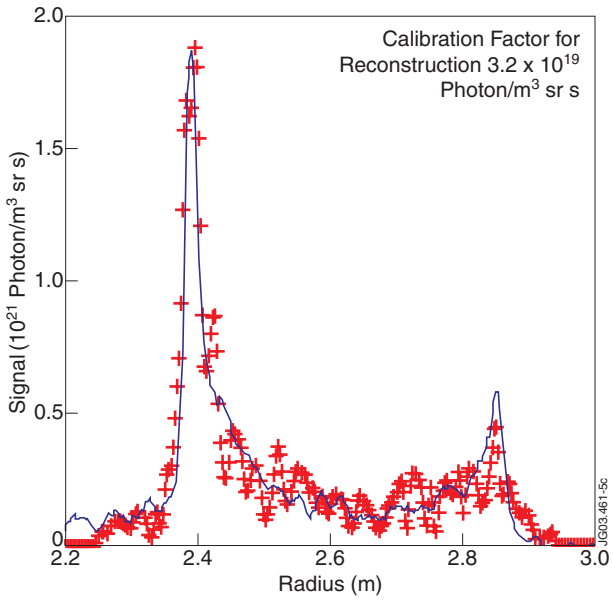

Figure 5: Comparison of reconstructed and mesured (KL2B) D_a- emission profiles.